Molecular dynamics studies of atomic-scale friction for roller-on-slab systems with different rolling–sliding conditions

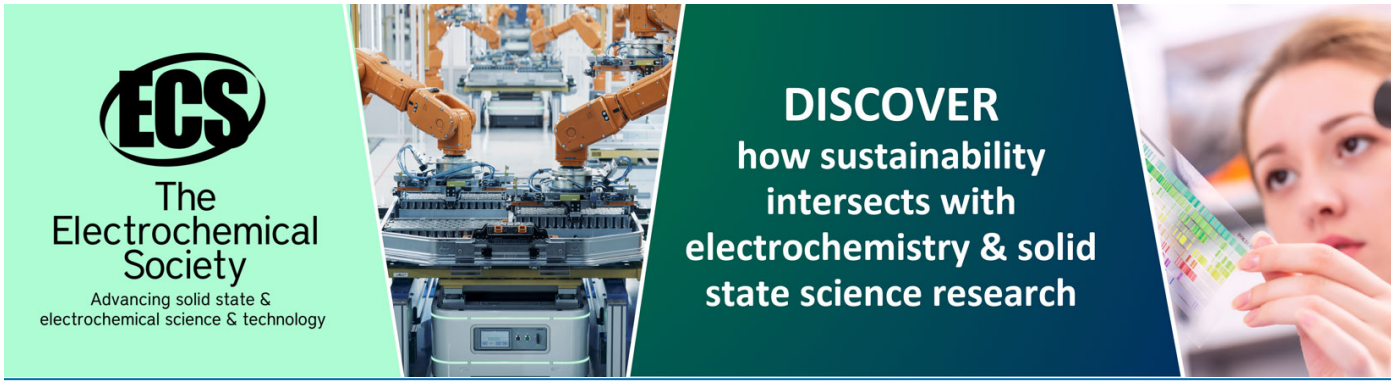

INSTITUTE OF PHYSICS PUBLISHING NANOTECHNOLOGY
Nanotechnology **16** (2005) 1941–1949 doi:10.1088/0957-4484/16/9/087

Molecular dynamics studies of atomic-scale friction for roller-on-slab systems with different rolling–sliding conditions

Yeau-Ren Jeng[1,3], **Ping-Chi Tsai**[1] **and Te-Hua Fang**[2]

[1] Department of Mechanical Engineering, National Chung Cheng University, Chia-Yi 621, Taiwan
[2] Institute of Mechanical and Electromechanical Engineering, National Formosa University, Yunlin 632, Taiwan

E-mail: imeyrj@ccu.edu.tw

Received 1 November 2004, in final form 28 June 2005
Published 28 July 2005
Online at stacks.iop.org/Nano/16/1941

Abstract
This paper presents the use of molecular dynamics (MD) simulations to investigate atomic-scale frictional behaviour between a roller and a slab under rolling–sliding conditions. The simulations consider both abrasive wear and non-abrasive wear during the rolling–sliding process. Different rolling–sliding conditions are simulated by implementing various separation distances between the roller and the slab and by changing the angular velocity of the roller. The frictional and normal forces acting at the interface between the roller and the slab, and the temperature of both operating components, are calculated during the rolling–sliding process. The relationships between the roller–slab friction phenomena and the rolling–sliding conditions are investigated. Finally, the rolling–sliding characteristics associated with a hard-on-soft rolling–sliding system are compared with those of a soft-on-soft rolling–sliding system.

1. Introduction

Tribological studies play a fundamental role in improving the operating performance of components used at the nanometric level [1–9]. Many such studies have been performed to investigate the mechanisms of atomic-scale sliding friction between two contact surfaces, either experimentally using atomic force microscopy (AFM) and friction force microscopy (FFM) techniques, or theoretically via molecular dynamics simulations [10]. The effects on sliding friction of the applied load, crystallographic sliding direction, temperature, and sliding velocity have been studied for various materials [11–14]. It is well known that the sliding friction which occurs during machinery operation results in power loss, component wear, and temperature rise. As a result, the performance of the machining system is compromised and the lives of its components shortened. Various investigations of atomic-scale sliding friction have been carried out under different sliding conditions [15–25]. However, relatively few studies have conducted detailed investigations into the full range of rolling–sliding behaviours. From a macroscopic viewpoint, if sliding between two contact surfaces is replaced by a rolling motion, for example by the use of roller bearings [6, 11], the effects of sliding friction on the working components are reduced significantly. Taking the microscopic viewpoint, it is known that an object is comprised of atoms or molecules and is neither a continuous nor a rigid body [12, 26–38]. Therefore, a rolling motion does not actually take place between the two contact surfaces. Consequently, reducing the sliding friction at the microscopic scale is more complex than in the macroscopic case. Hence, improving the operating performance of nanoscale components demands that serious attention be paid to reducing atomic sliding friction between the contact surfaces.

This study establishes a classical molecular dynamics roller–slab model to investigate atomic-scale friction effects

[3] Author to whom any correspondence should be addressed.

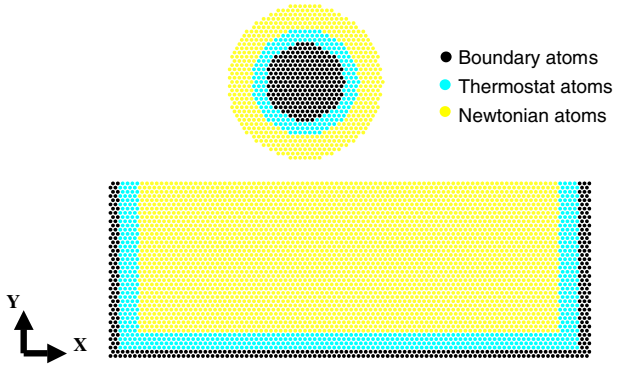

Figure 1. The atomic roller–slab model for MD simulations. (This figure is in colour only in the electronic version)

during the rolling–sliding process. In the simulations, the separation distance between the roller and the slab and the angular velocity of the roller are varied in order to simulate different rolling–sliding conditions. This study has identified the rolling–sliding conditions which minimize sliding friction. An assumed rolling condition, referred to as quasi-rolling, is proposed. Under this condition, the linear velocity at the bottom of the roller is equal to 0 unit when the roller is regarded to be a rigid body. This simulation adopts the Morse potential to calculate the interatomic forces between the various atoms. Hard-on-soft and soft-on-soft rolling–sliding systems are established to simulate abrasive and non-abrasive wear conditions, respectively.

The frictional and normal forces acting on the interface between the roller and the slab, and the temperature of both operating components, are calculated during both rolling–sliding processes. The effects of the separation distance and the angular velocity on the frictional phenomena are investigated. Finally, the sliding behaviour of the hard-on-soft rolling–sliding system is compared with that of the soft-on-soft system.

2. Simulation methodology

Figure 1 shows the two-dimensional roller–slab model simulated in the present study. The atomic arrangement is consistent with the (111) crystal plane of face-centred-cubic (fcc) lattice materials [13]. The proposed model comprises three kinds of atoms, namely boundary, thermostat, and Newtonian. The boundary atoms are assumed to be unaffected by the indentation and rolling–sliding process. Consequently, they are fixed in their initial lattice positions and serve to reduce the edge effects and maintain the proper symmetry of the lattice. The motions of the thermostat atoms are modified based on the Nosé–Hoover method [39]. This procedure is used to simulate the thermostatic effects of the bulk and guarantee the equilibrium temperature to approach the desired value since much of the cutting heat converted from strain energy and friction energy will be carried away by chip and lubricant in actual rolling–sliding conditions. The motions of the Newtonian atoms are determined by the interatomic forces produced by the interaction potential and direct solution of Newton's motion equation. Thus, the interactions between the slab and the roller can be studied using this approach.

Table 1. Number of atoms of each type used in present MD simulations.

Rolling/sliding system	Hard-to-soft		Soft-to-soft	
Components	Roller	Slab	Roller	Slab
Rigid atoms	223	499	236	499
Thermostat atoms	210	666	198	666
Newtonian atoms	480	3114	492	3114
Total	913	4279	926	4279

Table 2. Morse potential parameters.

	Slab	Roller	Roller/slab
D (eV)	$0.3429_{(\mathrm{Soft})}$ [a]	$2.423_{(\mathrm{Hard})}$ [b] $0.3429_{(\mathrm{Soft})}$	0.1
α (nm)	$13.588_{(\mathrm{Soft})}$	$25.55_{(\mathrm{Hard})}$ $13.588_{(\mathrm{Soft})}$	17
r_0 (nm)	$0.2626_{(\mathrm{Soft})}$	$0.2626_{(\mathrm{Soft})}$ $0.2522_{(\mathrm{Hard})}$	0.22

[a] Soft indicates that the parameter is used in soft material.
[b] Hard indicates that the parameter is used in hard material.

As shown in figure 1, the boundary atoms are arranged such that they form a U-shaped boundary around the slab. Similarly, the thermostat atoms arranged inside the rigid atoms also have a U-shaped arrangement. Meanwhile, the Newtonian atoms occupy the region bounded by the U-shaped isothermal layer and are free to move across the upper surface of the slab under the influence of interactive forces supplied by the surrounding atoms. Regarding the roller, the boundary, thermostat, and Newtonian atoms are arranged into three concentric annuli, as shown in figure 1. In both operating components, the boundary atoms form fixed boundaries across which the thermostat and Newtonian atoms cannot pass. It is noted that the radius of the roller is constant throughout the various rolling–sliding simulations. Table 1 details the total number of atoms of each kind within the present hard-on-soft and soft-on-soft rolling–sliding simulation systems. Meanwhile, the Morse potential [27, 28] is employed to calculate the atomic interactive forces between the atoms. The Morse potential is written as

$$\phi(r_{ij}) = D\{\exp[-2\alpha(r_{ij} - r_0)] - 2\exp[-\alpha(r_{ij} - r_0)]\} \quad (1)$$

where $\phi(r_{ij})$ is a pair potential energy function, and D, α, and r_0 correspond to the cohesion energy, the elastic modulus and the atomic distance at equilibrium, respectively. The Morse potential parameters adopted in this study are shown in table 2 [36]. In addition, the force on atom i resulting from the interaction of all the other atoms can be derived from the above potential function, equation (1), such that

$$F_i = -\sum_{\substack{j=i \\ (j\neq i)}}^{N} \nabla_i \phi(r_{ij}) = m_i \frac{\mathrm{d}^2 r_i\,(t)}{\mathrm{d}t^2} \quad (2)$$

where F_i is the resultant force on atom i, m_i is the mass of atom i, r_i is the position of atom i, and N is the total number of atoms. Initial velocities are assigned from the Maxwell

distribution, and the magnitudes are adjusted so as to keep the temperature in the system constant according to

$$v_i^{\text{new}} = \left\{ \frac{3NK_{\text{B}}T_0}{2} \left[\sum_{i=1}^{N} \frac{m_i (v_i^{\text{old}})^2}{2} \right]^{-1} \right\}^{\frac{1}{2}} v_i^{\text{old}} \qquad (3)$$

where v_i is the velocity of atom i, T_0 is a specified temperature, k_{B} is Boltzmann's constant ($=1.381 \times 10^{-23}$ J K^{-1}), and N is the total number of atoms. However, the initial displacement and velocity are values determined independently; the time integration of motion is performed by the fifth Gear's predictor–corrector method [13, 40–42]. The Morse potential has been selected for these simulations because it is relatively simple, and it has been used for several similar studies previously. We expect it to be adequate for the qualitative investigation of the rolling–sliding phenomena described here.

The current study considers the hard-on-soft and soft-on-soft rolling–sliding systems to represent atomic abrasive and non-abrasive wear conditions, respectively. In the hard-on-soft rolling–sliding system, the dissociation energy of the roller exceeds that of the slab by more than seven times. Conversely, in the soft-on-soft roller–slab system, the roller and the slab possess identically small dissociation energies. Diamond (C) and copper (Cu) are chosen as the hard and soft materials, respectively, for which the Morse potential parameters adopted in this study are listed in table 2.

The present MD simulations were conducted in three stages, as follows.

(1) Atoms other than the boundary atoms were relaxed from their initial positions to assume an equilibrium configuration under the interaction of atomic forces at 300 K.
(2) The roller was rotated with a specified angular velocity and displaced downwards toward the slab until the designated separation distance between the roller and the slab was attained.
(3) The roller was moved with a constant linear and angular velocity along the [110] direction of the (111) crystal plane of the slab.

For each rolling–sliding simulation, the travel distance of the roller was specified to be 5.252 nm (2×10^5 time steps) and the linear velocity of the centre of the roller was fixed at a constant 36 m s^{-1}. In this study, different rolling–sliding conditions were simulated by changing both the angular velocity of the roller and the separation distance between the roller and the slab. To evidently investigate the effect of the angular velocity on the deformation, the frictional phenomena and the temperature of roller/slab during rolling–sliding process, the larger order of the angular velocity (the magnitude of 10^{10} rad s^{-1}) has been employed, and the comparable angular velocity was varied in the range of -2.7×10^{10} to 1.8×10^{10} rad s^{-1}. It is noted that an angular velocity of -0.9×10^{10} rad s^{-1} in both operating components (i.e. hard-on-soft and soft-on-soft rolling–sliding systems) during the rolling–sliding process is the so-called quasi-rolling condition. In addition, it is necessary to note that the angular velocities in this study are many orders of magnitude higher than experimental angular velocities. This is due to the computational intensity of the congenital problem; many of these simulations were restricted to smaller model sizes or to very high velocities, or to both. However, the present molecular dynamic simulations are nevertheless adequate for generating qualitative estimates. Based on the changes of the normal force during indentation [43], the relationship between the interactive force field and the separation distance can be described as follows: (1) repulsive force field: 0.2 nm, −0.3 and −0.8 nm, (2) attractive force field: 0.45 nm, (3) non-interactive force field: 0.7 nm. Therefore, in order to simulate different interactive force fields between the two operating components, three initial interface distances between the bottom of the roller and the top surface of the slab (i.e. separation distances) were considered, namely −0.7, −0.2, and 0.3 nm.

The objective of the present MD simulations was to investigate the effects of the roller angular velocity and separation distance parameters on the normal and frictional forces acting between the roller and the slab and the effects of these parameters on the temperatures of the two operating components. It is interesting to note that the microscopic definitions of the normal and frictional forces are very broad and can include much variation, therefore, we would like to better clarify the distinction between normal and frictional forces for nanoscale components. In this study, we have proposed that microscopic contacts and bumps on surfaces cause frictional forces. When two surfaces contact each other, tiny bumps on each of the surfaces tend to run into each other, preventing the surfaces from moving past each other smoothly. The frictional force is obtained by the force in the sliding direction, which is defined as the X-direction. In contrast, the normal force is determined from the force in the Y-direction. In addition, the slab and roller temperatures are obtained by calculating the total kinetic energy (i.e. the friction and the strain energy) of constituent Newtonian atoms. Although some cutting heat will be carried away by the chip, there is still some heat built up at the roller/slab interface.

3. Results and discussion

3.1. Effect of separation distance between roller and slab

3.1.1. Deformation and wear of roller and slab. Figures 2(a) and (b) show the atomic positions of the roller and slab during the hard-on-soft and soft-on-soft rolling–sliding processes, respectively, for various values of angular velocity and a constant separation distance of −0.7 nm. In each case, the simulation results are presented for x-direction displacements of 0 nm (0 time step), 2.626 nm (1×10^5 time steps), and 5.252 nm (2×10^5 time steps). The results reveal that in both rolling–sliding systems, deformation and wear of the two operating components increase as the displacement of the roller across the surface of the slab increases. In the hard-on-soft rolling–sliding system (figure 2(a)), the rolling–sliding process is similar to that of a milling process executed with a machining centre. The roller of the hard-on-soft rolling–sliding system can be regarded as a rigid body, and hence abrasive wear is restricted almost entirely to the slab surface. Therefore, atoms around the slab surface are displaced from their original positions as the roller travels across the surface. Although the results are deliberately omitted in this paper, rolling–sliding

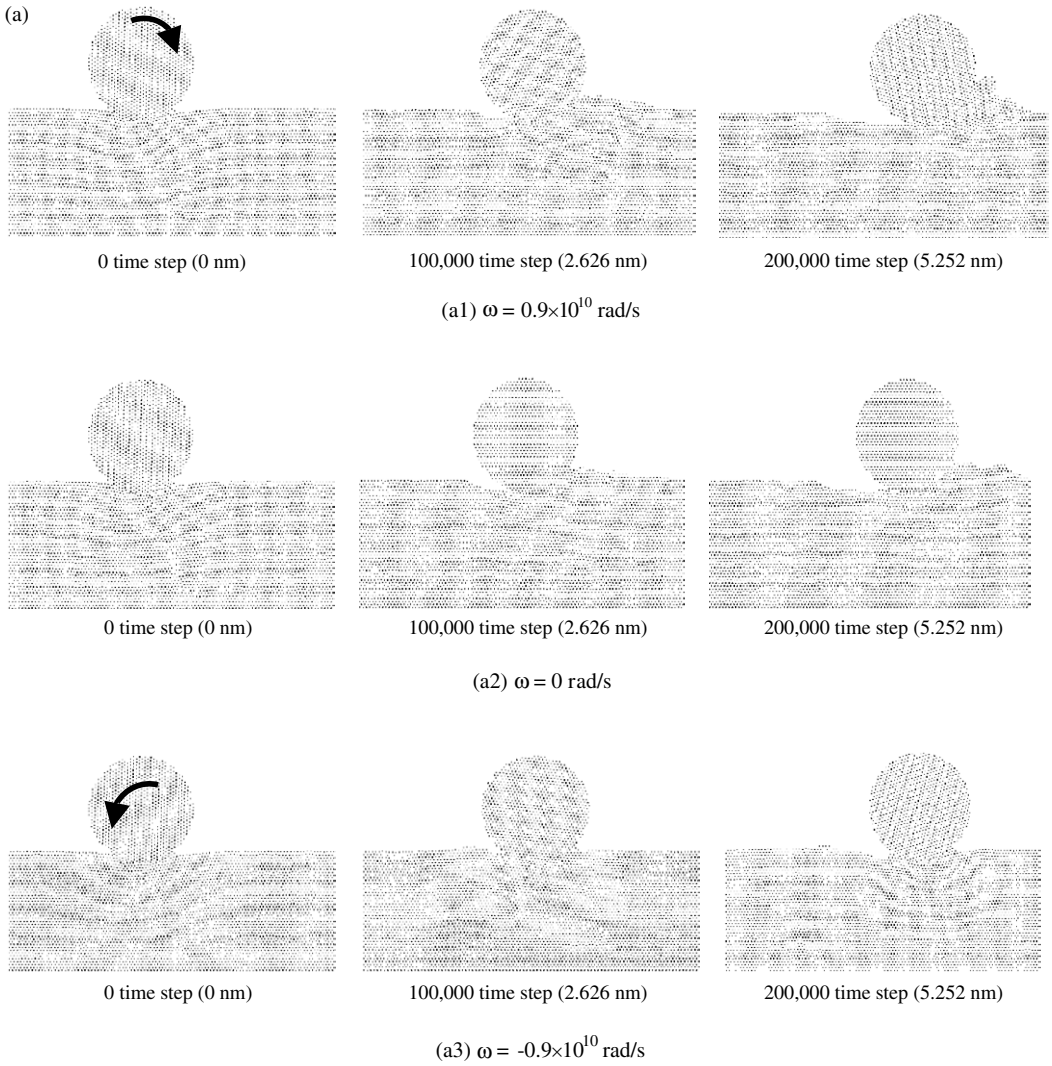

Figure 2. Atomic positions of roller and slab during rolling–sliding processes for a roller with different angular velocities and a constant separation distance of −0.7 nm at different time steps. (Note that $\omega = 0.9 \times 10^{10}$ rad s^{-1} has a clockwise rotation. Comparatively, $\omega = -0.9 \times 10^{10}$ rad s^{-1} has a counterclockwise rotation.) (a) Hard-on-soft roller–slab system and (b) soft-on-soft roller–slab system.

simulations were also conducted at separation distances of −0.2 and 0.3 nm. It was noted that, at a separation distance of −0.2 nm, only marginal chip and deformation were evident in the two operating components, even though a slight *y*-direction indentation of the roller into the slab occurred. Therefore, the current simulation results suggest that deformation and wear of the roller and slab are more pronounced when the separation distance exceeds −0.2 nm. In addition, in the soft-on-soft rolling–sliding system (figure 2(b)), the stick and slip are clearly observed for a large number of close-packed contact surfaces. This observation can be attributed to the lower cohesion energy, which reduces the robustness of the roller in the soft-on-soft rolling–sliding system. Regarding the surface–surface contact, this similar phenomenon is in good agreement with that reported by Sørensen *et al* [44], although the tool geometry is somewhat different.

3.1.2. Normal force and frictional force on roller/slab interface. Figure 3 shows the variation of the normal force with the separation distance for various values of roller angular velocity in the hard-on-soft and soft-on-soft rolling–sliding systems. An observation of the normal force variation in both systems reveals that the atomic interactive forces between the roller and the slab can be divided into three distinct force fields, namely non-interactive, attractive, and repulsive. As stated above, the current study considered three separation distances, i.e. 0.3, −0.2, and −0.7 nm. As shown in figure 3, the normal force acting at separation distances of −0.2 and −0.7 nm is positive, which indicates that a repulsive force field exists between the roller and the slab. Furthermore, in both rolling–sliding systems, it is noted that, regardless of the angular velocity of the roller, this positive normal force is inversely proportional to the separation distance until this distance reduces to approximately −0.2 nm. When the separation distance is less than −0.2 nm, the variations of the normal force are affected by the angular velocity of the roller and by its direction. However, in both rolling–sliding systems, the effects of the angular velocity of the roller on the normal force are irregular, and are hence difficult to evaluate

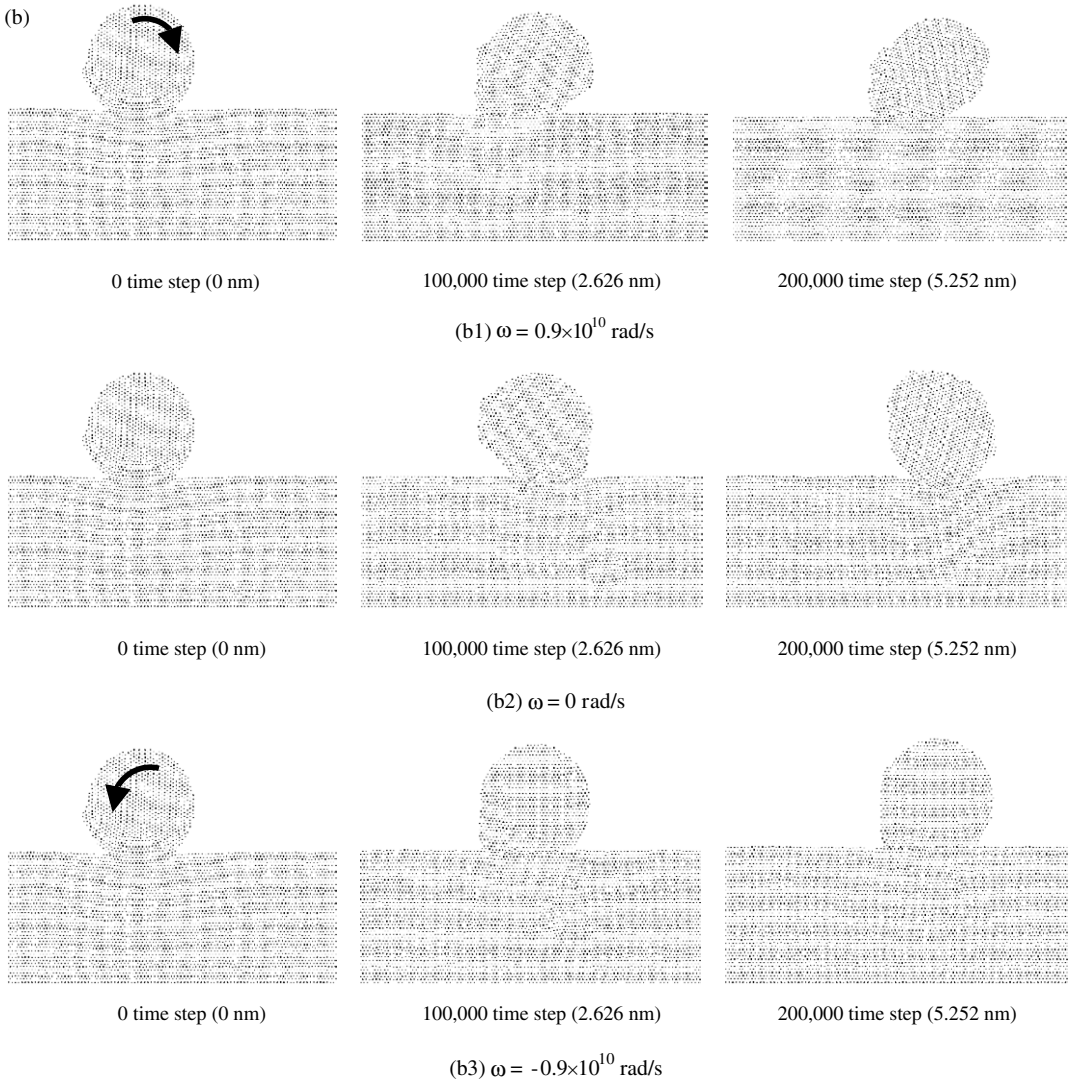

Figure 2. (Continued.)

during the indentation operation. When a separation distance of 0.3 nm is applied during the rolling–sliding process, the interactive force between the roller and the slab is an attractive force. For both rolling–sliding systems, the attractive force field prompts several atoms to be attracted away from the slab surface towards the roller. Figure 3 also reveals that the normal force maintains a constant value of approximately zero for separation distances greater than 0.6 nm in both rolling–sliding systems. This is indicative of a non-interactive force field. Hence, at these separation distances, it can be concluded that the effects of the angular velocity on the normal force are insignificant in both rolling–sliding systems. Consequently, the normal force generated during indentation is influenced primarily by the separation distance between the roller and the slab.

Figure 4 shows the variation of the frictional force with the separation distance for various values of roller angular velocity during the indentation operation. In both rolling–sliding systems, it is observed that, regardless of the angular velocity value, the frictional force maintains a value of approximately zero until the roller moves to a separation distance of 0.2 nm. However, when the separation distance is less than 0.2 nm, the amplitudes of the frictional force in the hard-on-soft rolling–sliding system are greater than those in the soft-on-soft rolling–sliding system. In other words, the frictional force on roller/slab interface depends on the cohesion energy of the Morse potential (i.e. the robustness of the roller). This similar phenomenon also is virtually all in good agreement with the previous studies by Maekawa *et al* [29] for machining induced by pure sliding conditions, where it demonstrates that the interface has larger cutting forces, frictional forces, and temperature as the bond energy has been increased. Specifically, during the indentation operation, a greater rotational resistance at the interface between the roller and the slab is observed in the case of the hard-on-soft rolling–sliding system. It is noted that the influence of frictional force is clearly apparent even though the roller and the slab do not make contact with each other. Figure 4 reveals that with the exception of an angular velocity of -0.9×10^{10} rad s^{-1}, the frictional force clearly increases with increasing roller angular velocity in both rolling–sliding systems.

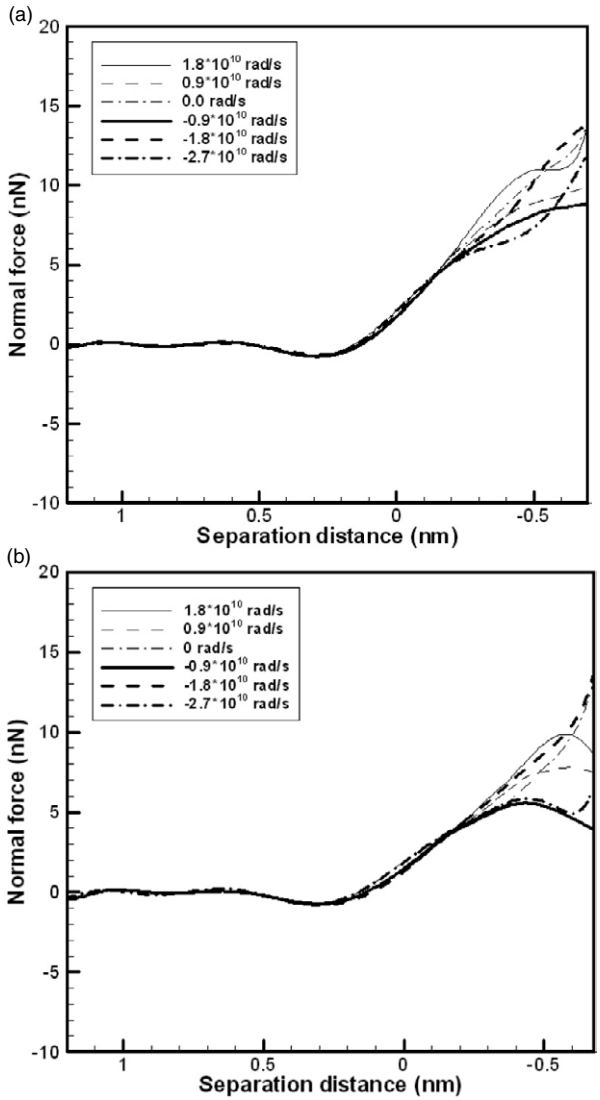

Figure 3. Variation of normal force with separation distance for a roller with different angular velocities during indentation operation. (a) Hard-on-soft rolling/sliding system and (b) soft-on-soft rolling/sliding system.

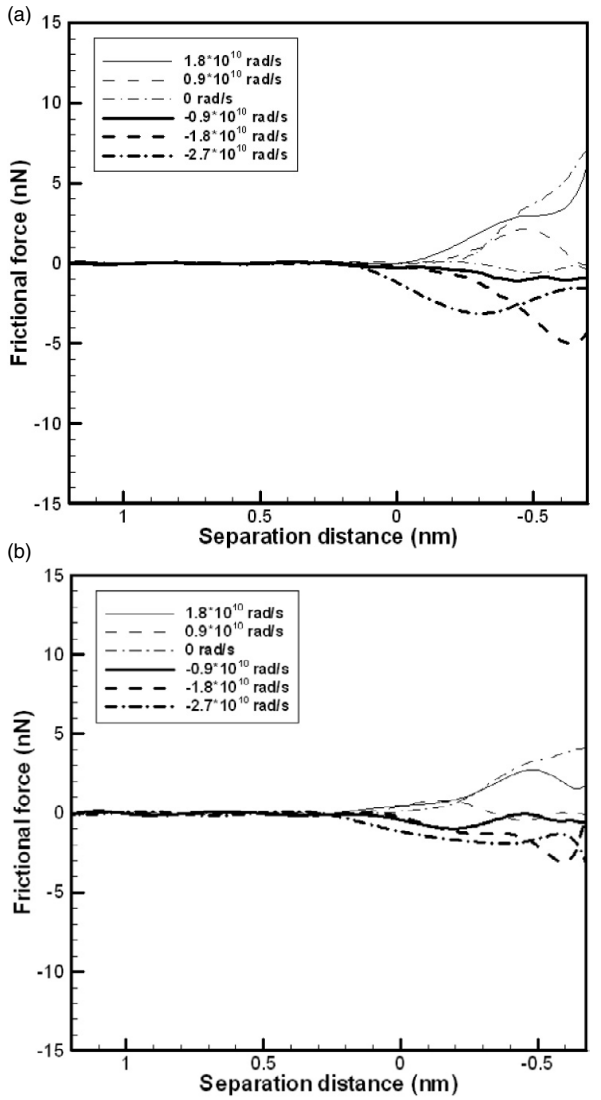

Figure 4. Variation of frictional force with separation distance for roller with different angular velocities during the indentation operation. (a) Hard-on-soft rolling/sliding system and (b) soft-on-soft rolling/sliding system.

3.2. Effects of angular velocity between roller and slab

3.2.1. Deformation and wear of roller and slab. Figure 2(a) reveals that in the hard-on-soft rolling–sliding system, deformation and wear of the slab surface increase with increasing roller angular velocity other than when the angular velocity exceeds 0.9×10^{10} rad s^{-1} or is lower than -1.8 rad s^{-1}. Under these exceptional conditions, it is observed that the roller remains virtually fully intact. For reasons of clarity, figure 2 presents the results only for angular velocities of 0, 0.9×10^{10} and -0.9×10^{10} rad s^{-1}. As shown in figure 2, for the hard-on-soft rolling–sliding system, the slab wear accumulates in front of the roller when the roller rotates in the positive direction (counterclockwise) or when it travels with zero angular velocity. Conversely, when the roller rotates in the negative direction (clockwise), the slab wear accumulates at the tail of the roller. In the soft-on-soft rolling–sliding system, this same effect is observed when the roller travels with either a positive or a zero angular velocity. In the soft-on-soft rolling–sliding system, although deformation and wear occur simultaneously, their effects are restricted primarily to the roller. It is observed that the roller deformation increases with increasing angular velocity. This observation is attributed to the larger contact arc between the roller and the slab which exists at higher angular velocities. Furthermore, when the roller rotates with an angular velocity of -0.9×10^{10} rad s^{-1}, minimum wear and deformation of the slab surface is evident in both rolling–sliding systems, while in the soft-on-soft rolling–sliding system, the roller deformation is significantly reduced. Therefore, under a repulsive force field, the quasi-rolling condition results in lower deformation and wear after completion of the rolling–sliding operation in both the hard-on-soft and soft-on-soft rolling–sliding systems.

3.2.2. Normal force and frictional force on the roller/slab interface. Figure 3 shows that the effect of the angular

velocity on the normal force is insignificant compared to the influence of the separation distance in both rolling–sliding systems. However, the frictional force increases with increasing angular velocity, as shown in figure 4. Comparing the normal force with the frictional force, the normal force can act in two opposite directions depending on the particular force field in effect, i.e. non-interactive, attractive, or repulsive, during the rolling–sliding process, whereas the direction of the frictional force is determined solely by the rotational direction of the roller. Figures 2 and 4 illustrate that an angular velocity of -0.9×10^{10} rad s^{-1} results in a lower deformation and wear of both operating components. The present study defines this condition as a quasi-rolling condition. Moreover, it is also observed that a relatively smaller normal force acts on the interface between the roller and the slab under this particular rolling condition. Previously, Jeng *et al* [43] proposed a slider–slab model to investigate atomic-scale sliding friction, in which they demonstrated that lower deformation and wear of the sliding components result in a smaller value of the normal force and the frictional force during sliding. Therefore, the present results are in agreement with previous studies by Jeng *et al*. Additionally, the current results indicate that an angular velocity of zero leads to maximum values of the absolute normal force and frictional force in both rolling–sliding systems. This result is attributed to the fact that the roller does not rotate but purely slides on the slab, hence leading to a maximum sliding resistance at the interface between the two operating components in both rolling–sliding systems. The simulation results for the normal force and the frictional force clearly indicate that the minimum absolute resistance at the interface depends not only on the angular velocity of the roller, but also on the separation distance between the roller and the slab in both rolling–sliding systems. Finally, the results suggest that the optimum angular velocity of -0.9×10^{10} rad s^{-1} minimizes both the normal force and the frictional force to attain less wear and deformation. Therefore, when performing an atomic-scale milling process, the use of a tool rotating with a negative angular velocity minimizes wear and deformation at the interface between the tool and the workpiece.

3.3. Effects of angular velocity and separation distance on temperature of roller/slab during rolling–sliding process

Figures 5 and 6 show the effects of the angular velocity and separation distance on the average temperatures of the slab and roller, respectively. As shown in figure 5(a), the average slab temperature increases with decreasing separation distance and with increasing roller angular velocity in the hard-on-soft rolling–sliding system. Under these indentation conditions, the Newtonian atoms in the slab receive the external energy generated by the frictional force and by the normal force, and hence their total kinetic energies increase in both rolling–sliding systems. Moreover, since the roller rotates with an angular velocity during indentation, the Newtonian atoms in the slab also receive rotational energy, which further increases their total kinetic energies. In the soft-on-soft rolling–sliding system, the angular velocity of the roller has relatively little effect on the average slab temperature, as shown in figure 5(b). Meanwhile, figure 6(a) shows that in the hard-on-soft rolling–sliding system, the angular velocity of the roller

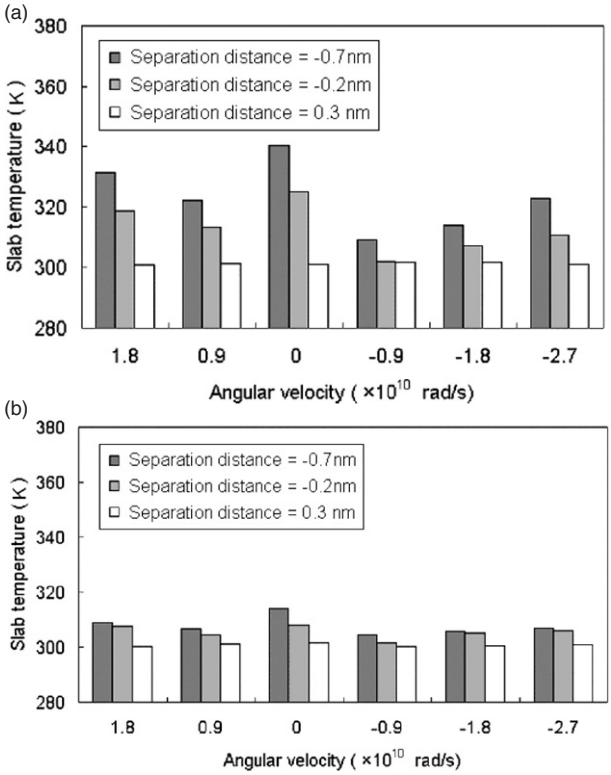

Figure 5. Average slab temperature as a function of different angular velocities on the roller at separation distances of 0.3, −0.2 and −0.7 nm. (a) Hard-on-soft rolling–sliding system and (b) soft-on-soft rolling–sliding system.

has relatively little influence on the average roller temperature. A comparison of figures 5 and 6 indicates that in the hard-on-soft rolling–sliding system, the highest temperature occurs on the slab surface, whereas in the soft-on-soft rolling–sliding system, the highest temperature occurs in the roller. This observation demonstrates that the regions of serious wear and deformation exhibit a higher temperature during the rolling–sliding process. It is noted that the temperature of the slab in the hard-on-soft system, and the temperature of the roller in the soft-on-soft system, attain a maximum value when the angular velocity of the roller is equal to zero. When the roller does not rotate but simply slides across the surface of the slab, the resulting increased normal and frictional forces supply a greater external energy to the Newtonian atoms of the operating components, which in turn increases their temperatures. A similar behaviour has also been reported by Bhushan *et al* for dry sliding conditions [9].

In the quasi-rolling condition, if the roller is assumed to be a rigid body which rotates with an angular velocity of -0.9×10^{10} rad s^{-1}, the velocity at the bottom point of the roller is equal to zero. The rigid roller and the slab will then exhibit a purely rolling condition during the rolling–sliding process. However, from a microscopic perspective, it is known that a pure rolling condition does not actually occur since the two objects are comprised of atoms or molecules. Therefore, the present study adopts an approximate rolling condition, referred to as the quasi-rolling condition. In this study, when the roller rotates with an angular velocity of

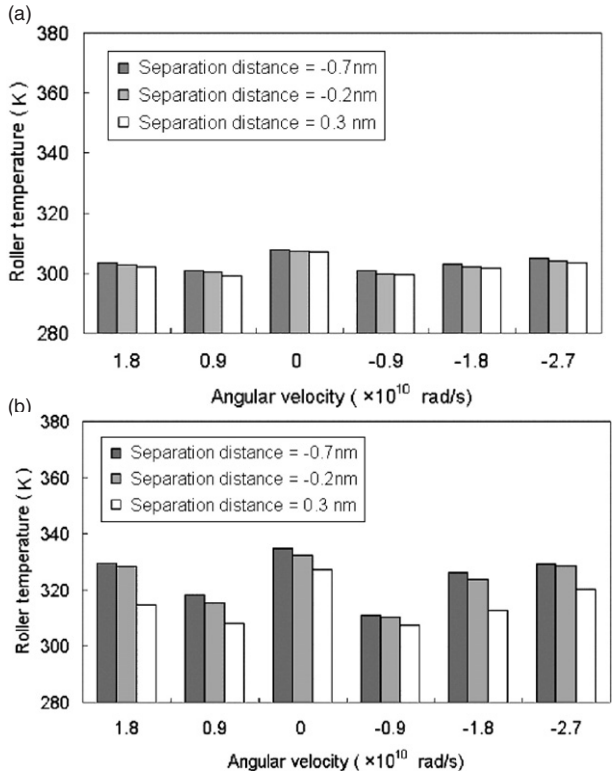

Figure 6. Average roller temperature as a function of different angular velocities on the roller at separation distances of 0.3, −0.2 and −0.7 nm. (a) Hard-on-soft rolling–sliding system and (b) soft-on-soft rolling–sliding system.

-0.9×10^{10} rad s^{-1}, the rolling–sliding process is regarded to be a quasi-rolling process and both rolling–sliding systems exhibit the following set of characteristics. Under the repulsive force field:

(1) minimum deformation and wear of the two working components is observed following a complete rolling–sliding operation,
(2) the normal and frictional forces acting at the interface between the roller and the slab are minimized, and
(3) the average slab temperature and average roller temperature are minimized.

Meanwhile, under the attractive force field, the atomic interactive force between the roller and the slab is small. Therefore, in the quasi-rolling condition, there is virtually no difference between the hard-on-soft and soft-on-soft rolling–sliding conditions in terms of the effects of the separation distance and angular velocity on the slab temperature and atomic movements.

4. Conclusions

This study has established a roller–slab model to investigate atomic-scale frictional phenomena. A hard-on-soft and a soft-on-soft rolling–sliding system have been proposed to simulate abrasive and non-abrasive wear conditions, respectively. The Morse potential has been utilized to calculate the interactive force between the atoms. The angular velocity of the roller and the separation distance between the roller and the slab have been varied in order to simulate different rolling–sliding conditions. The principal conclusions of the present study can be summarized as follows.

(1) In both rolling–sliding systems, the wear and deformation of the two operating components increase with reducing separation distance and with increasing angular velocity of the roller, with the exception of an angular velocity of -0.9×10^{10} rad s^{-1}.
(2) From a consideration of normal and frictional forces, the rolling–sliding system presented in this study more accurately reflects the atomic-milling process than systems which only consider pure sliding.
(3) The present atomic-scale rolling–sliding simulation defines an angular velocity of -0.9×10^{10} rad s^{-1} as a quasi-rolling condition and has shown that this condition generates lower wear and deformation and reduced temperature increases in both rolling–sliding systems.

Acknowledgments

The authors gratefully acknowledge the support provided to this research by the National Science Council, Taiwan. NSC93-2120-M-194-006 and NSC93-2120-M-194-003. The support of AFOSR under contract No. F62562-03-P-0378 is also acknowledged.

References

[1] Bhushan B, Israelachvili J N and Landman U 1995 *Nature* **374** 607
[2] Kim D E and Suh N P 1994 *J. Tribol.* **116** 225
[3] Yan W and Komvopoulos K 1998 *J. Tribol.* **120** 385
[4] Bhushan B *et al* 1999 *Handbook of Micro/Nano Tribology* ed B Bhushan (Boca Raton, FL: Chemical Rubber Company Press)
[5] Landman U and Luedtke W D 1993 *MRS Bull.* (May) 36
[6] Landman U, Luedtke W D and Ringer E M 1992 *Wear* **153** 3
[7] Landman U, Luedtke W D and Gao J 1996 *Langmuir* **12** 4514
[8] Landman U 1998 *Solid State Commun.* **107** 693
[9] Bhushan B and Nosonovsky M 2004 *Nanotechnology* **15** 749
[10] Mate C M, McClelland G M, Erlandsson R and Chiang S 1987 *Phys. Rev. Lett.* **59** 1942
[11] Schofer J and Santner E 1998 *Wear* **222** 74
[12] Sundararajan S and Bhushan B 1999 *Wear* **229** 678
[13] Hail J M 1992 *Molecular Dynamics Simulation: Elementary Methods* (New York: Wiley)
[14] Tersoff J 1986 *Phys. Rev. Lett.* **56** 632
[15] Finnis M W and Sinclair J E 1984 *Phil. Mag.* A **50** 45
[16] Daw M S and Baskes M I 1983 *Phys. Rev. Lett.* **50** 1285
[17] Baskes M I 1992 *Phys. Rev.* B **46** 2727
[18] Harrison J A, White C T, Colton R J and Brenner D W 1992 *Phys. Rev.* B **46** 9700
[19] Harrison J A, Colton R J, White C T and Brenner D W 1993 *Wear* **168** 127
[20] Harrison J A, White C T and Colton R J 1995 *Thin Solid Films* **260** 205
[21] Harrison J A, White C T, Colton R J and Brenner D W 1993 *MRS Bull.* (May) 50
[22] Perry M D and Harrison J A 1996 *Langmuir* **12** 4552
[23] Perry M D and Harrison J A 1996 *Thin Solid Films* **290** 211
[24] Zhu H P and Yu A B 2003 *Physica* A **325** 347
[25] Yoshida A and Fujii M 2003 *Tribol. Int.* **36** 361

[26] Perry M D and Harrison J A 1997 *J. Phys. Chem.* B **101** 1364
[27] Shimada S, Ikawa N, Ohmori G, Tanaka H and Uchikoshi U 1992 *Ann. CIRP* **41** 117
[28] Shimada S, Ikawa N, Tanaka H and Uchikoshi U 1993 *Ann. CIRP* **42** 91
[29] Maekawa K and Itoh A 1995 *Wear* **188** 115
[30] Zhang L and Tanaka H 1997 *Wear* **211** 44
[31] Komanduri R, Chandrasekaran N and Raff L M 1998 *Wear* **219** 84
[32] Komanduri R, Chandrasekaran N and Raff L M 2000 *Wear* **240** 113
[33] Rentsch R and Inasaki I 1994 *Ann. CIRP* **43** 327
[34] Isono Y and Tanaka T 1996 *Trans. Japan. Soc. Mech. Eng.* **62** 2364
[35] Isono Y and Tanaka T 1999 *JSME Int. J.* A **42** 158
[36] Fang T H and Weng C I 2000 *Nanotechnology* **11** 148
[37] Lipkowitz K B and Boyd D B 1995 *Reviews in Computational Chemistry* vol 6 (New York: VCH)
[38] Gear C W 1971 *Numerical Initial Value Problems in Ordinary Differential Equations* (Englewood Cliffs, NJ: Prentice-Hall)
[39] Hoover W G 1985 *Phys. Rev.* A **31** 1695
[40] Rapaport D C 1995 *The Art of Molecular Dynamics Simulation* (Cambridge: Cambridge University Press)
[41] Heermann D W 1990 *Computer Simulation Methods* (New York: Springer)
[42] Frenkel D and Smit B 1996 *Understanding Molecular Simulation: from Algorithms to Applications* (San Diego, CA: Academic)
[43] Jeng Y R, Tsai P C and Fang T H 2005 *Tribol. Lett.* **18** 315
[44] Sørensen M R, Jacobsen K W and Stoltze P 1996 *Phys. Rev.* B **53** 2101